# REPORT No. 619

## DRAG OF CYLINDERS OF SIMPLE SHAPES

By W. F. Lindsey

### SUMMARY

*In order to determine the effect of shape, compressibility, and Reynolds Number on the drag and critical speed for simple forms, the drag forces on models of various simple geometric cross sections were measured in the N. A. C. A. 11-inch high-speed wind tunnel.*

*The models were circular, semitubular, elliptical, square, and triangular (isosceles) cylinders. They were tested over a speed range from 5 percent of the speed of sound to a value in excess of the critical speed, corresponding, for each model, approximately to a tenfold Reynolds Number range, which extended from a minimum of 840 for the smallest model to a maximum of 310,000 for the largest model.*

### INTRODUCTION

The aerodynamic drag of simple forms was one of the earliest subjects of aerodynamic research. Although numerous investigations have been conducted, drag data for many forms, especially as affected by Reynolds Number and compressibility, are incomplete or have never been obtained. In accordance with a suggestion made at one of the annual engineering conferences, tests to investigate the variation of drag for various simple forms with Reynolds Number were considered for the variable-density wind tunnel. There was available, however, a large amount of data on the drag of fundamental shapes that had been obtained under conditions involving rather large and uncertain turbulence effects. It was therefore considered preferable to transfer the investigation to the 11-inch high-speed tunnel, where disturbing turbulence effects were much smaller and where new information could be obtained concerning compressibility effects.

Previous investigations of the drag of simple forms have included the effects of Reynolds Number on the drag of circular cylinders (references 1 and 2), the effect of compressibility on the drag of circular cylinders (reference 3), the variation of drag with angle of attack for square cylinders (reference 4), the drag of flat plates normal to the wind (reference 4), and tests of elliptical cylinders of various fineness ratios. Test results, however, were not available for either triangular or semitubular cylinders, nor were any previous in-vestigations available that included the effects of compressibility on the drag characteristics of any of these forms, except the circular cylinder (reference 3).

The present investigation, comprising measurements of the drag of cylinders having various cross sections, was conducted over a range extending from 5 percent of the speed of sound to a speed above the value at which the compressibility burble occurred. This speed range corresponded, for each model, approximately to a tenfold Reynolds Number range, which extended from 840 to 8,400 for the smallest model and from 31,000 to 310,000 for the largest model.

The experiments were conducted from 1933 to 1936 in the N. A. C. A. 11-inch high-speed wind tunnel.

### APPARATUS AND METHODS

The N. A. C. A. 11-inch high-speed wind tunnel, in which the tests were made, is an induction-type closed-throat tunnel having a circular air passage. The tunnel is equipped with a balance, which is of the three-component, photorecording, spring type. The balance was designed for testing airfoils at speeds from approximately 35 percent of the velocity of sound to a speed approaching the velocity of sound. A detailed description of the tunnel and of the photo-recording balance is given in reference 5.

For some of the tests reported herein, the photo-recording balance was not sufficiently sensitive to measure the drag, and an auxiliary drag balance was therefore used. This balance was of the pendulum type and was designed to measure very small drag forces on small models at low speeds. The forces were measured by visual observation of the movement of a beam. Three balance sensitivities were used; a 1-inch deflection equaled 0.01 pound, 0.10 pound, or 1.0 pound. By the variation of the sensitivity and by the addition of counterweights, forces were measured from a minimum of 0.001 pound to a maximum of 10 pounds. One of the features incorporated in the construction of the balance was a means for applying tension to the model in order to overcome vibration difficulties encountered with some of the models in portions of the speed range.

The models tested were (a) circular, (b) semitubular, (c) elliptical, (d) square, and (e) triangular (isosceles) cylinders. The shapes and the dimensions of the cross sections are shown in figure 1. Because of the small size of the models and the relatively large forces involved, the models were constructed of steel. The surfaces were highly polished, and the edges of the semitubular, the square, and the triangular cylinders were sharp.
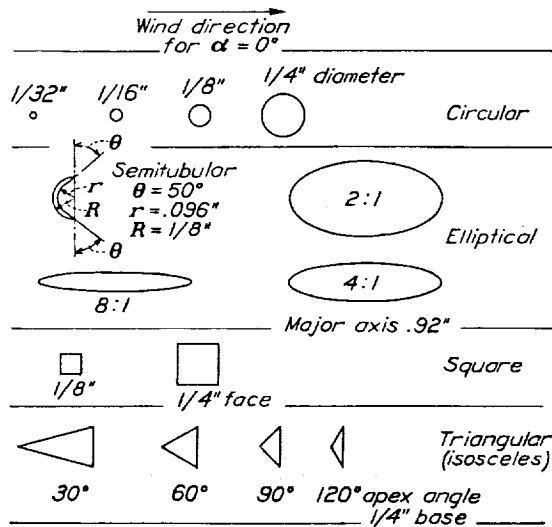


FIGURE 1.—Cross sections of cylinders.

The models were so mounted that they extended across the tunnel and passed through holes in the tunnel wall. These holes were covered with circular end plates of thin brass, which fitted into recesses in the tunnel wall and maintained the contour of the walls. Holes of the same shape but slightly larger than the model were cut in the end plates and provided a small clearance so that the end plates and the model did not touch. Previous investigations indicated that the results so obtained approximate infinite-aspect-ratio data.

The tests were conducted over a speed range from 5 percent of the speed of sound to a value above the speed at which the compressibility burble occurred.

The dynamic pressure, $\frac{1}{2}\rho V^2$, and the ratio of the velocity at the test section to the speed of sound at the test section, $V/V_c$, were determined from pressures measured at calibrated static-pressure orifices.

The areas used in computing the coefficients were taken as the product of a transverse dimension and the "effective span." The effective span, 10.93 inches, was determined from an impact-pressure survey across the tunnel. The computed coefficients are based on frontal area unless otherwise specified on the figures.

The angles of attack were measured from an arbitrarily chosen initial reference position ($\alpha=0°$), shown in figure 1 for each of the models.

## PRECISION

The various factors affecting the accuracy of these data may, in general, be divided into two classes: (a) accidental errors, and (b) systematic errors.

The accidental errors, indicated by the scatter of the test points on the curves, arose from slight changes in the calibrations of the balances and of the static-pressure orifices, from very small variations in the direction of the air flow, and from similar sources. The magnitude of these errors was estimated to be ±2 percent from an examination of the point scatter.

The systematic errors, arising from tunnel-wall effects and end interference, were impossible to evaluate without a special series of tests but, because the models were small in relation to the tunnel and tests of several sizes of circular cylinders indicated that the correction for the data presented is small, a correction was considered unnecessary.

## PRESENTATION OF DATA

The results are presented in the standard nondimensional coefficient form; that is, the force divided by the product of $\frac{1}{2}\rho V^2$ and the area. The area used in computing the coefficients is the frontal area, except as shown on the figures. The coefficients are plotted against the speed ratio $V/V_c$ and against Reynolds Number. Cross plots and summary plots of the data are included to facilitate analysis and for purposes of comparison.

The Reynolds Numbers for the data presented are based on the length of the model parallel to the wind direction, except for the semitubular cylinder for which the characteristic length, like that for the circular cylinder, is taken as the outside diameter.

## DISCUSSION

The resistance, or drag, coefficients of the various bodies depend on both Reynolds Number and compressibility. Because the turbulence of the tunnel air stream is small, the Reynolds Number almost entirely determines the flow pattern around the model at low speeds; whereas, at high speeds the compressibility effects become important and, ultimately, as the speed increases, become relatively so large that the Reynolds Number effects may, to a first approximation, be disregarded. Accordingly, throughout the discussion, Reynolds Number effects are considered as those changes in the coefficient that occur at low speeds and compressibility effects as those that occur at high speeds. Furthermore, the speed at which the flow breakdown occurs due to compressibility phenomenon is referred to as the "critical speed." Previous tests (reference 6) have demonstrated the critical speed to be that value of the translational velocity for which the

sum of the maximum induced velocity near the surface of the body and the translational velocity equals the local speed of sound. The flow change at the critical speed is called, in accordance with earlier terminology, the "compressibility burble."

The values of the critical speed indicated by the drag curves for the bodies investigated are less definite than the values indicated by drag curves for finely shaped bodies, such as airfoils, because the rise in drag at high speeds is not very sharp. For the circular cylinder, however, visual observations of the flow by means of the schlieren method were made, and these observations served as a guide in the selection of the value of the critical speed from the drag curves for the circular cylinders.

Circular cylinder.—The results from the tests of the drag of circular cylinders are presented in figures 2 and 3; the results as affected by Reynolds Number



FIGURE 4.—Variation in $C_{D_0}$ with $V/V_c$ for the semitubular cylinder.



FIGURE 2.—Variation in $C_{D_0}$ with $V/V_c$ for the circular cylinders.
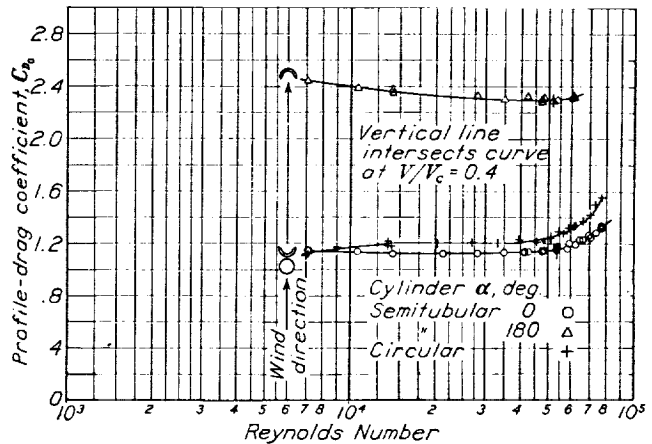


FIGURE 5.—Variation in $C_{D_0}$ with Reynolds Number for the semitubular cylinder.

(fig. 3) are in good agreement with Relf's results (reference 2).
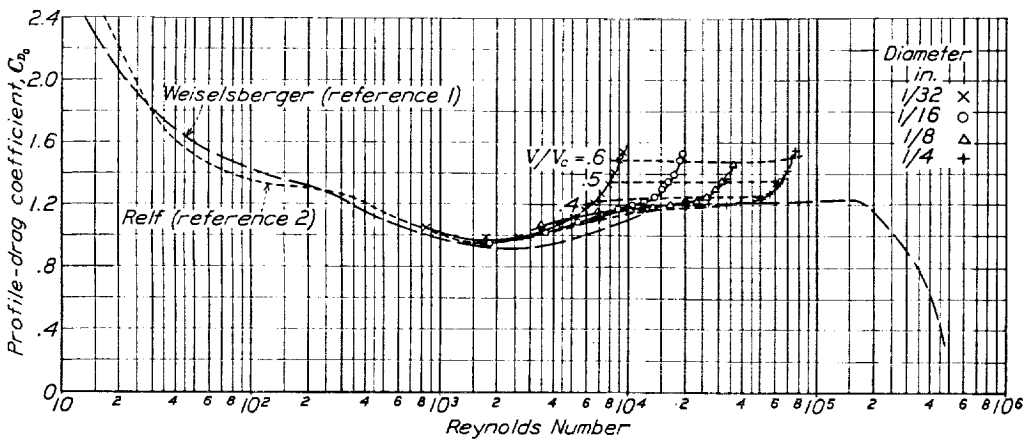


FIGURE 3.—Variation in $C_{D_0}$ with Reynolds Number for the circular cylinders.

Further, these tests indicate that the critical speed is independent of Reynolds Number within the range investigated. The critical speed for the circular cylinder at values of the Reynolds Numbers above the critical probably differs somewhat from that given herein because of the change in the pressure distribu-
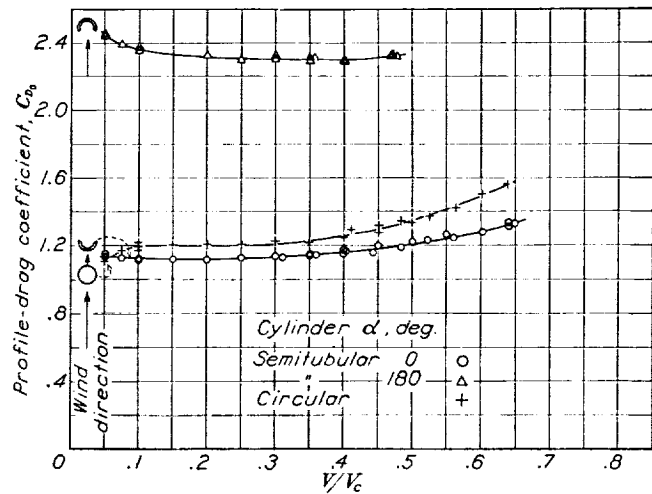
tion for the circular cylinder that occurs after the critical Reynolds Number is exceeded. The present results, however, indicate that the critical speed is unaffected by Reynolds Number for ranges wherein no marked changes in the flow pattern occur. Unfortunately, these tests could not be extended to higher values of the Reynolds Number because tests of larger cylinders indicated serious tunnel-wall effects that could not readily be evaluated.

For speeds higher than the critical, the test results (figs. 2 and 3) indicate the drag coefficient to be a function of the speed ratio, or compressibility index, $V/V_c$. This statement is not a general conclusion inasmuch as figure 3 shows that the Reynolds Number range corresponding to this speed range occurs within

the region where the drag coefficient is approximately constant.

**Semitubular cylinder.**—The data from the tests of the semitubular cylinder (figs. 4 and 5) indicate that the drag coefficient, when the concave surface is to the wind ($\alpha=180°$), is approximately twice as large as when the convex surface is to the wind ($\alpha=0°$). A large increase in drag would be expected from elementary considerations.
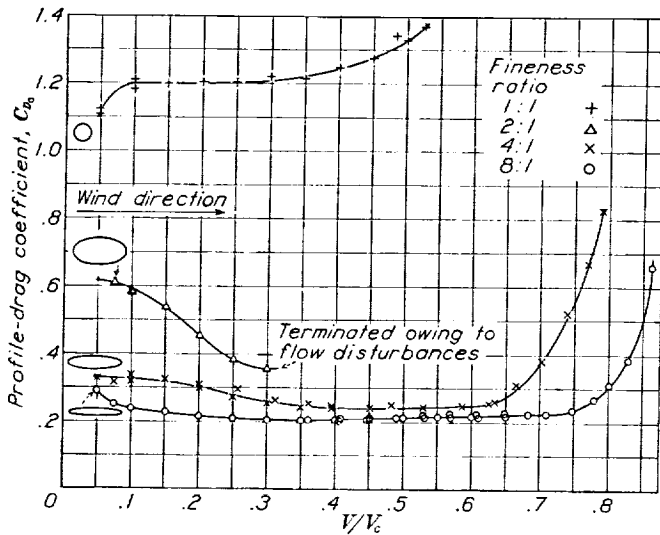


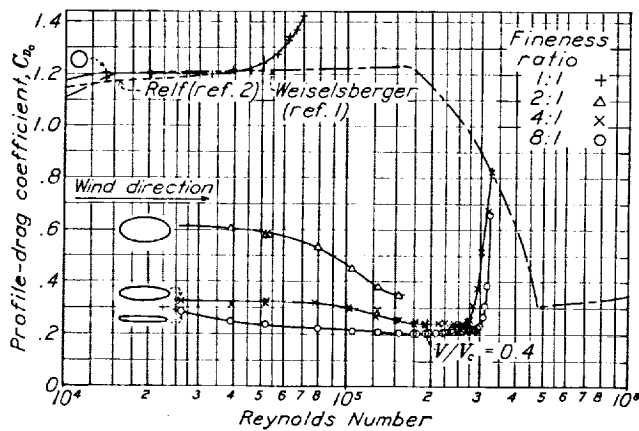FIGURE 6.—Variation in $C_{D_0}$ with $V/V_s$ for the elliptical cylinders.



FIGURE 7.—Variation in $C_{D_0}$ with Reynolds Number for the elliptical cylinders.

**Elliptical cylinder.**—A study of the compressibility effects on elliptical cylinders (figs. 6 and 7) shows a marked decrease in critical speed with decrease in fineness ratio. This result is to be expected from previous investigations since experiments have indicated (reference 6) that the compressibility burble occurs when the velocity at any point in the field of flow around the model exceeds a value corresponding to the local speed of sound, and investigations of the pressure distribution around elliptical cylinders (reference 7) show that the induced velocities decrease with increasing fineness ratio.

Relations between the fineness ratio and the critical speed can be obtained quantitatively from theoretical considerations. From the potential-flow theory, the induced pressure over the elliptical cylinder can be obtained from the equation

$$\frac{\Delta p}{q}=1-\frac{(a+b)^2y^2}{b^4+(a^2-b^2)y^2} \text{ (reference 8, equation (14))}$$

where $a$ is the semimajor axis.

    $b$, the semiminor axis.

    $\Delta p$, the difference between the undisturbed stream pressure and $p$, the pressure at the surface of the model.

    $y$, the ordinate from the major axis to the point of pressure, $p$.

For the maximum negative value of $\Delta p/q$, $y$ is equal to $b$. The equation easily reduces to the form $\left(\frac{\Delta p}{q}\right)_{max}=-t(2+t)$ where $t$ is the thickness-chord ratio. The relation between the maximum induced pressure $\left(\frac{\Delta p}{q}\right)_{max}$ (from low-speed tests or as calculated from the potential-flow theory for incompressible fluids) and the critical speed is developed and presented graphically in reference 9. The results from references 8 and 9 may be combined to give the relation between the critical speed and the thickness-chord ratio presented in figure 8. A comparison of the theoretical with the experimental results, also shown in figure 8, indicates
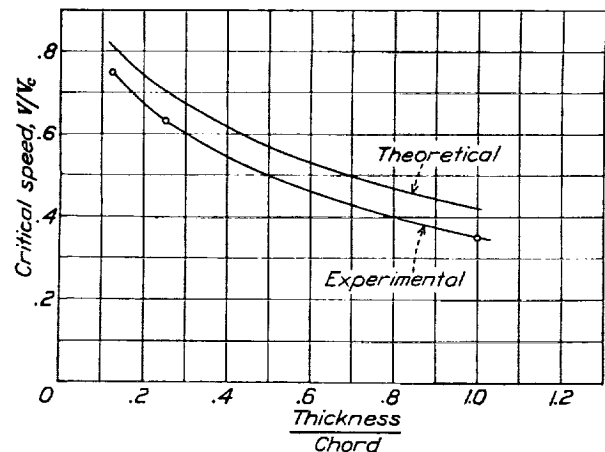


FIGURE 8.—Variation in critical speed with thickness-chord ratio for the elliptical cylinders.

that the theory gives a fair approximation of the critical speed for elliptical cylinders. The predicted values are somewhat high. Even higher values are obtained if, instead of the theoretically derived values, low-speed measurements of $\left(\frac{\Delta p}{q}\right)_{max}$ are used in computing the critical speeds.

As regards Reynolds Number effects, the results of tests of the model (fig. 7) having the highest fineness ratio (8:1) indicate no pronounced change in drag coefficient with Reynolds Number. With decrease in

fineness ratio to the 2:1 ellipse, however, the change becomes pronounced.

The results of Wieselberger's tests of circular cylinders of infinite aspect ratio (reference 1) are included in figure 7. A comparison of these results (considered as data for an elliptical cross section having a fineness ratio of 1:1 and obtained under conditions of turbulence either equal to or greater than the low turbulence of the 11-inch high-speed tunnel) and the results of the present investigation of the elliptical cross section having a fineness ratio of 2:1 indicates a decrease in critical Reynolds Number with increase in fineness ratio.
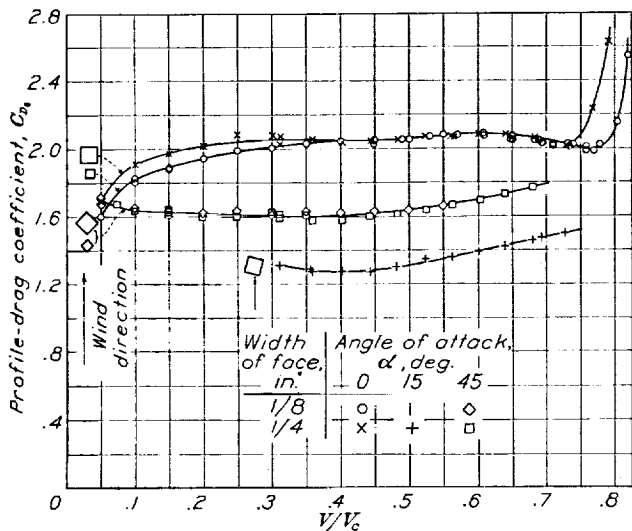
with a diagonal parallel to the wind. Inasmuch as the flow probably separates at the sharp edges for all values of the Reynolds Number, the pressure drag coefficient tends to remain constant and is such a large part of the total drag coefficient that the effect of Reynolds Number is relatively small.

For the square cylinders, face normal to the wind ($\alpha=0°$ in fig. 10), at the higher values of Reynolds Number, the drag coefficient is practically constant and approximates that of a flat plate set normal to the wind. At the lower values of the Reynolds Number, however, the drag coefficient appears to decrease with decreasing Reynolds Number; incomplete separation at the forward edges possibly causes this change.



FIGURE 9.—Variation in $C_{D_0}$ with $V/V_s$ for the square cylinders.



FIGURE 11.—Variation in $C_{D_0}$ with $V/V_s$ for the triangular cylinders.



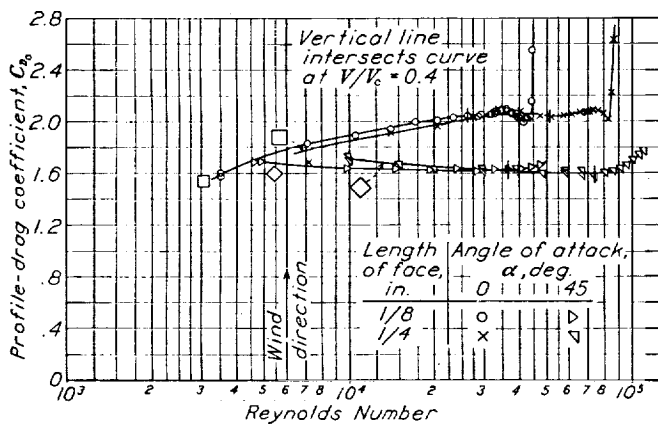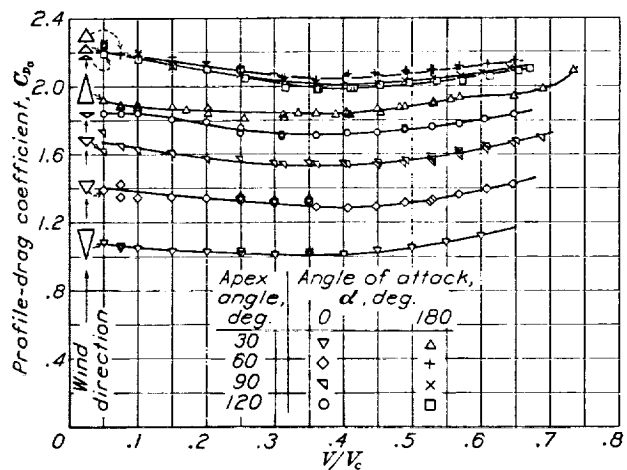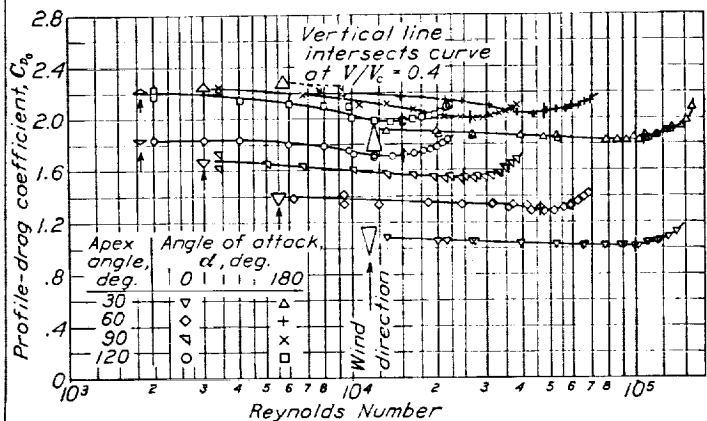FIGURE 10.—Variation in $C_{D_0}$ with Reynolds Number for the square cylinders.



FIGURE 12.—Variation in $C_{D_0}$ with Reynolds Number for the triangular cylinders.

Square cylinder.—The results of the drag tests at the various angles of attack for the square cylinders are presented in figures 9 and 10. These results indicate that the drag coefficient is smaller when a diagonal is parallel to the wind ($\alpha=45°$) than when the face of the model is normal to the wind ($\alpha=0°$). The total drag of models of the same size, however, is smaller at $\alpha=0°$ than at $\alpha=45°$.

Figure 10 indicates that there is but little Reynolds Number effect on the drag coefficient of the models

Within the Reynolds Number range investigated, no sudden changes in flow were indicated by the results of the tests at any of the angles of attack.

The compressibility effects for models with a diagonal parallel to the wind ($\alpha=45°$ in figs. 9 and 10) appear to be independent of Reynolds Number within the range investigated. This result is in general agreement with the results of the tests of circular cylinders.

Triangular cylinder.—The effect of the apex angle on the drag coefficient of triangular (isosceles) cylinders is

shown in figure 11. As the apex angle is increased and with either apex or base to the wind, the drag coefficient increases and approaches that of a flat plate normal to the wind, as is to be expected since the model tends to become a flat plate as the apex angle approaches 180°. With the base of the triangular cylinder to the wind, there is no appreciable effect on the drag coefficient from increasing the apex angle above a value of 60°. With the apex to the wind, however, there is a continuous increase in drag coefficient with increase in apex angle above 30°.

Reynolds Number has but little effect on the drag coefficient of models having triangular cross sections (fig. 12). The same characteristic is shown by the results from tests of models having square cross section with the diagonal parallel to the wind (fig. 10).

The compressibility effects (figs. 11 and 12) appear to be independent of apex angle and are the same for angles of attack of 0° (apex to the wind) and of 180° (base normal to the wind). The compressibility effects for both triangular (isosceles) cylinders and for square cylinders with a diagonal parallel to the wind direction ($\alpha = 45°$) are approximately the same.
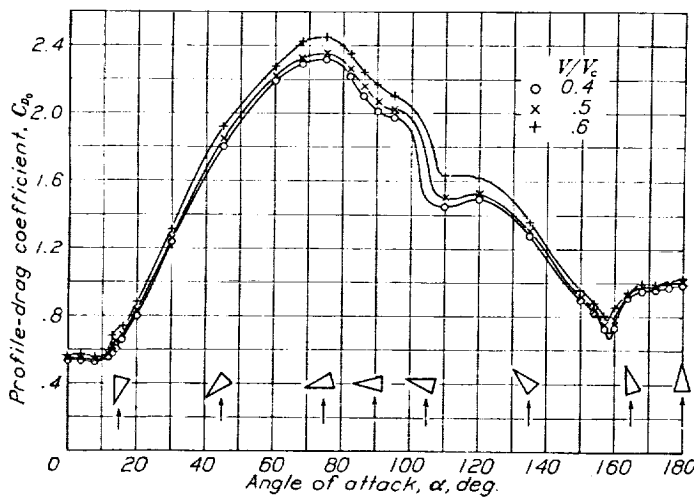


FIGURE 13.—Variation in $C_{D_0}$ with $\alpha$ for the triangular cylinder having an apex angle of 30°. Area=altitude×span.

The test results of figure 13 show the variation in drag coefficient, based on a constant area (product of altitude and effective span), with angle of attack for each of several values of the speed ratio $V/V_c$. Each curve indicates, for a particular value of the speed ratio $V/V_c$, the variation in total drag for a triangular cross section having an apex angle of 30°. The maximum drag occurs when one of the long sides is normal to the wind, the condition corresponding to an angle of attack of 75°.

The results indicate abrupt changes in the flow pattern within certain ranges of angle of attack, as evidenced by the sudden changes in drag coefficient. It is of interest to note that, at or near these critical

angles of attack, one of the long sides of the model becomes either parallel or perpendicular to the direction of the wind, as illustrated by figure 13.

The variation in drag coefficient with the speed ratio for several representative angles of attack is presented in figure 14 to show the compressibility effects. Apparently the compressibility effects are greater at or near the critical angle-of-attack ranges, as indicated by steeper slopes of the curves in figure 14 and by the vertical displacement of the curves in figure 13.
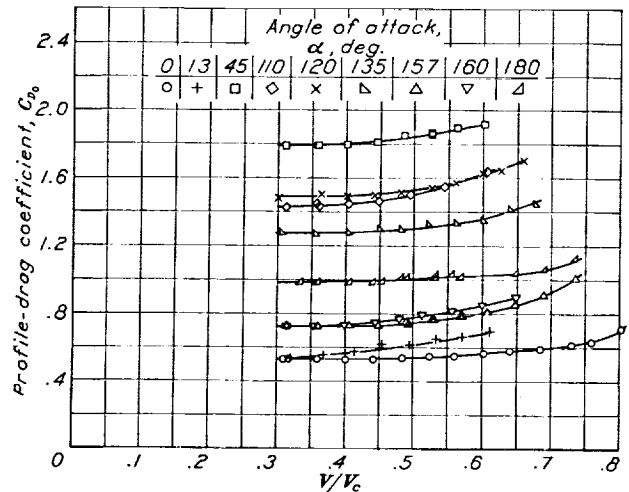


FIGURE 14.—Variation in $C_{D_0}$ with $V/V_c$ for the triangular cylinder having an apex angle of 30°. Area=altitude×span.

The variation in lift coefficient with angle of attack is shown in figure 15 for three values of the speed ratio, $V/V_c$. The results show that sudden variations in the lift coefficient occur in the same critical angle-of-attack ranges in which the drag coefficient changes, a further indication that there are abrupt changes in the flow pattern. The variation in lift coefficient with $V/V_c$ for angles of attack within the critical angle-of-attack range is presented in figure 16.

An extrapolation of the drag coefficient of triangular cylinders having various apex angles with the base to the wind is presented in figure 17, in which the drag coefficient is plotted against the ratio of altitude to base $h/b$ for each of several values of the speed ratio, $V/V_c$. As $h/b$ approaches zero, the triangular section approaches an infinitely thin flat plate set normal to the wind. Thus, the extrapolation of the results of tests of models having triangular cross sections to a value of $h/b = 0$ should give a good estimate of the drag coefficient for flat plates of infinite aspect ratio set normal to the wind. The drag coefficient, obtained from this extrapolation, decreases slightly with increase in Reynolds Number. At equal Reynolds Numbers based on width normal to the stream, the extrapolated results are in good agreement with values from German tests conducted over limited Reynolds Number and speed ranges (reference 4).

**Effect of shape on drag.**—Figure 18 illustrates the relative drag of all the models and shows the general effect of shape on the drag coefficient. The drag coefficient, based on frontal area for all the models, is plotted against the speed ratio, $V/V_c$. The sizes of



FIGURE 15.—Variation in $C_L$ with $\alpha$ for the triangular cylinder having an apex angle of 30°. Area=altitude×span.



FIGURE 16.—Variation in $C_L$ with $V/V_c$ for the triangular cylinder having an apex angle of 30°. Area=altitude×span.

the models were consistent in that the frontal areas were approximately equal. The drag coefficient of the N. A. C. A. 0012–63 airfoil (reference 10) is included for comparison.

The agreement in drag coefficient between the semitubular cylinder with convex surface to the wind ($\alpha=0°$) and the circular cylinder is reasonably close and is to be expected in this Reynolds Number range because separation occurs in front of the central plane. At values of the Reynolds Number above the critical value, however, a greater difference in drag coefficient for the two forms is to be expected because the separation occurs back of the central plane for the circular
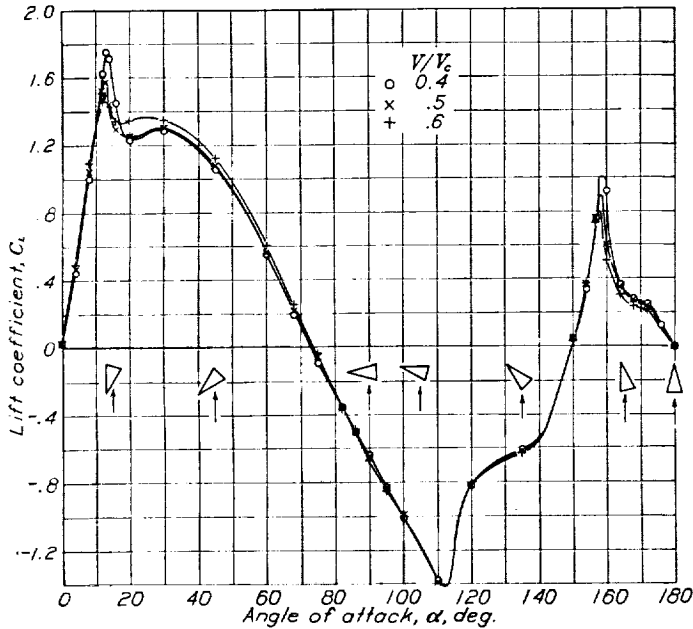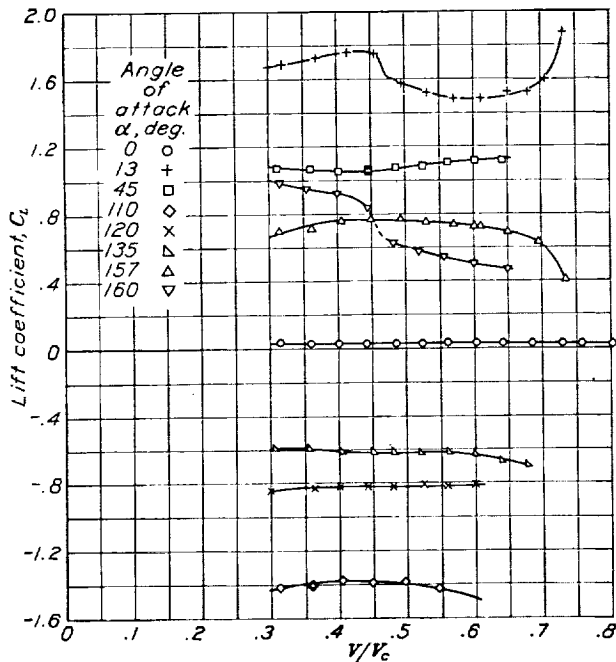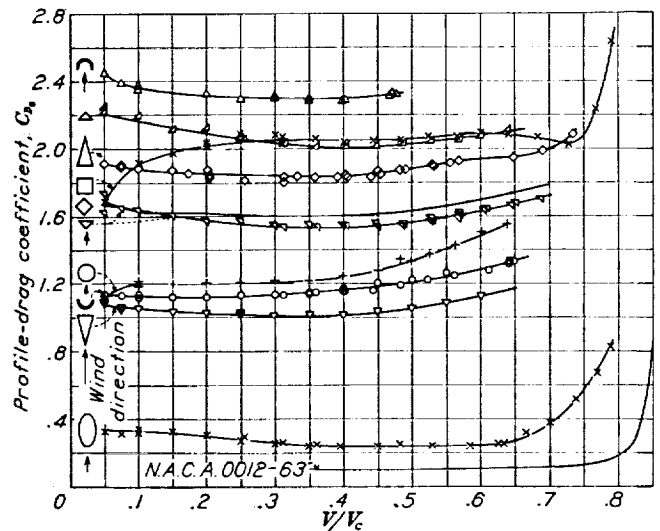


FIGURE 17.—Extrapolation for $C_{D_0}$ of flat plates normal to the wind.



FIGURE 18.—Effect of shape on $C_{D_0}$.

cylinder and at the central plane for the semitubular cylinder.

Similarly, the drag coefficient of the triangular cylinder having a 90° apex angle with the apex to the wind is only slightly less than the drag coefficient of the square cylinder with a diagonal parallel to the wind. This condition of approximately equal drag coefficients is to be expected because the point of separation is fixed for both forms at the sharp edges.

In general, the data show that, except for the square cylinder with a face normal to the wind, the higher-drag bodies have, in general, less rapid rise in drag coefficient at the higher speeds.

## CONCLUSIONS

1. The compressibility effects appear to be independent of Reynolds Number for ranges wherein there are no marked changes in the flow pattern caused by Reynolds Number effects.

2. The critical speed of elliptical cylinders decreases with decrease in fineness ratio.

3. For bodies having sharp edges that may be expected to define the separation point, the Reynolds Number effects are small. This result substantiates earlier investigations.

LANGLEY MEMORIAL AERONAUTICAL LABORATORY,
NATIONAL ADVISORY COMMITTEE FOR AERONAUTICS,
LANGLEY FIELD, VA., *October 27, 1937*.

## REFERENCES

1. Wieselsberger, C.: New Data on the Laws of Fluid Resistance. T. N. No. 84, N. A. C. A., 1922.
2. Relf, E. F.: Discussion of the Results of Measurements of the Resistance of Wires, with Some Additional Tests on the Resistance of Wires of Small Diameter. R. & M. No. 102, British A. C. A., 1914.
3. Stanton, T. E.: On the Effect of Air Compression on Drag and Pressure Distribution in Cylinders of Infinite Aspect Ratio. R. & M. No. 1210, British A. R. C., 1929.
4. Wieselsberger, C.: Der Widerstand verschiedener Körper. Ergebnisse der Aerodynamischen Versuchsanstalt zu Göttingen. II. Lieferung, 1923, S. 33–34.
5. Stack, John: The N. A. C. A. High-Speed Wind Tunnel and Tests of Six Propeller Sections. T. R. No. 463, N. A. C. A., 1933.
6. Stack, John: The Compressibility Burble. T. N. No. 543, N. A. C. A., 1935.
7. Parsons, John F., and Wallen, Jarvis A.: An Investigation of the Phenomenon of Separation in the Air Flow around Simple Quadric Cylinders. T. N. No. 354, N. A. C. A., 1930.
8. Zahm, A. F.: Flow and Drag Formulas for Simple Quadrics. T. R. No. 253, N. A. C. A., 1927.
9. Jacobs, Eastman N.: Methods Employed in America for the Experimental Investigation of Aerodynamic Phenomena at High Speeds. Misc. Paper No. 42, N. A. C. A., 1936.
10. Stack, John, and von Doenhoff, Albert E.: Tests of 16 Related Airfoils at High Speeds. T. R. No. 492, N. A. C. A., 1934.